Electronic Supplementary Material (ESI) for Journal of Materials Chemistry B.


# Supporting Information

## Tuneable redox-responsive albumin-hitchhiking drug delivery to tumour for cancer treatment

Shiwei Fu,[a] Ajay Zheng,[a] Lukun Wang,[a] Jiuyan Chen,[a] Bowen Zhao,[a] Xiao Zhang,[a] Victoria A. A. Mckenzie,[a] Zixin Yang,[a] Roger M. Leblanc,[a] Rajeev Prabhakar and Fuwu Zhang*[ab]

[a] Department of Chemistry, University of Miami, Coral Gables, FL 33146, USA

[b] The Dr. John T. Macdonald Foundation Biomedical Nanotechnology Institute, University of Miami, Miami, FL 33136, United States.

*Corresponding author: Fuwu Zhang: fxz174@miami.edu

## Experimental section

**Material.** All the chemicals were purchased and used as received unless otherwise noted. DM1 was purchased from Matrix Scientific (Columbia, SC, USA). 3-Mercaptopropionic acid, 16-Mercaptohexadecanoic acid, N-Hydroxysuccinimide, 4-dimethylaminopyridine (DMAP), and all the anhydrous solvents were purchased from Sigma-Aldrich (St. Louis, MO, USA). 3-Maleimidopropionic acid, 1,2-di(pyridine-2-yl) disulfane was purchased from AmBeed (Arlington Hts, IL, USA). 3-(3-Dimethylaminopropyl)-1-ethyl-carbodiimide hydrochloride was purchased from Chem-Impex (Wood Dale, IL, USA). All NMR solvents were used as received from Cambridge Isotope Laboratories, Inc. Dulbecco's Modification of Eagle's Medium (DMEM) with 4.5 g/L glucose, L-glutamine and sodium pyruvate (catalog number: 10-013-CV), 0.25% trypsin with 2.21 mM EDTA (catalog number: 25-0530-CI), and Dulbecco's Phosphate Buffered Silane (DPBS) (catalog number: 21-020-CV) were purchased from Corning. Penicillin-Streptomycin solution (catalog number: SH40003.01) was purchased from Cytiva. Thiazolyl blue tetrazolium bromide (MTT, catalog number: 158990010) was purchased from Acros Organics. Dimethyl Sulfoxide (DMSO) was purchased from Fisher Chemical. All the reagents were used without further purification.

**Instrumentation.** NMR spectra were recorded on an Avance Bruker 500 MHz spectrometer. Mass spectra was recorded with a Bruker MicroQ-TOF ESI mass spectrometer. Dynamic light scattering (DLS) measurements and the particle zeta potential values were determined using a Malvern ZEN1600 (MALVERN, Ltd., Worcestershire, UK). HPLC was performed on a Shimadzu HPLC system (LC-20AT) connected with PDA detector (SPD-M20A) and fluorescence detector (RF-20A). MTT

absorption was measured on Perkin Elmer Victor3 multi-label readers at $\lambda_{abs}$ = 570 nm.

**Kinetic binding assay of EB-ss-DM1 with BSA by Isothermal Titration Calorimetry (ITC).** Isothermal titration calorimetry (ITC) experiments were carried out using a Nano-ITC (New Castle, DE, USA). Bovine serum albumin (BSA) was dissolved in 1x PBS buffer to obtain a 10 μM solution. The EB-ss-DM1 prodrugs were diluted to a concentration of 100 μM. All solutions were extensively degassed for 10 min. In a typical experiment, the cell contained 0.5 ml of a solution of 10 μM BSA and the syringe contained ~100 μl of EB-ss-DM1 solution (100 μM). Titrations were performed as follows: 20 injections of 5 μl (EB-ss-DM1). The cell was stirred at 250 r.p.m. The delay time between the injections was 200 seconds. Data were analyzed using NanoAnalyze software fitting them to a single binding site model.

**In vitro drug release.** The decrease of EB-ss-DM1 prodrugs was measured by HPLC. Briefly, EB-ss-DM1-3 or EB-ss-DM1-16 in water were diluted with phosphate buffered saline (PBS) or the PBS with different concentrations of glutathione (GSH) for 24 h, yielding a concentration of 20 μg/mL, respectively. The decrease of EB-ss-DM1 concentration was monitored by HPLC (condition: acetonitrile (5%-95%) and water (95%-5%), UV detector at 254 nm, 20 μL/each time).

***In vitro*** **cytotoxicity assays.** The 4T1 murine mammary cancer cells (RPMI-1640), AsPC-1 (RPMI-1640), and PANC-1 (DMEM) were plated in 96-well plates (3 x $10^3$ cells/well) in medium (10% fetal bovine serum and 1% penicillin/streptomycin), respectively. Cells were incubated at 37 °C in a humidified atmosphere containing 5% $CO_2$ atmosphere. The culture medium was replaced with serial dilutions of EB-ss-DM1

(100 μL) in fresh medium and incubated for 72 h. The medium was then replaced with 100 μL medium containing 3-(4,5-dimethylthiazol-2-yl)-2,5-diphenyltetrazolium (MTT). After 3 h incubation, the medium containing unreacted MTT was carefully removed, and the obtained blue formazan crystals were dissolved in 100 μL DMSO. The absorbance at 570 nm was measured by SpectraMax i3x. The cell viability was calculated based on the relative absorbance to untreated cells (100% cell viability) and control medium (no cells, 0% cell viability).

***In vitro*** **cellular uptake investigation.** 4T1 cells were seeded into a glass bottom dish (dish diameter 35 mm, glass diameter 14 mm) which contained 900 μL of RPMI-1640 in each well at a density of $6 \times 10^4$ cells/well. Following a 24 hour-incubation, the medium was substituted with fresh RPMI-1640 containing a concentration of 10 μM of either EB-ss-DM1-3 or EB-ss-DM1-16. The control was prepared with the same volume of fresh medium without the prodrug. The cells were then incubated for 2 h, fixed by 4% paraformaldehyde (PFA) for 15 min, and stained by 1 μg/ml Hoechst 33342 solution for 10 min at room temperature. Finally, the cell imaging was performed on a Zeiss 880 confocal microscope. The PANC-1 cells were seeded in a glass-bottom dish (dish diameter 35 mm, glass diameter 14 mm) at a density of $1 \times 10^5$ cells per well. After incubation of 24 h, the medium was replaced with fresh DMEM containing 10 μM of either EB-ss-DM1-3 or EB-ss-DM1-16. The control was prepared with the same volume of fresh medium without the prodrug. The cells were then incubated for 2 h, fixed by PFA, stained by Hoechst 33342 solution, and imaged by confocal microscope.

**Computational details.** The ligand model was developed utilizing the high-resolution X-ray structure (PDB ID: 2BXH).[1] Indoxyl sulfate, present in the PDB structure, was excluded, and the human serum albumin protein underwent a 100ns equilibration using molecular dynamics with the GROMACS 2022 package and Amber 14 parmbsc1 force field.[2-5] Substrates EB-ss-DM1-3 and EB-ss-DM1-16 were utilized, and their charges and electrostatic potentials were computed at the b3lyp/6-311G(d,p) level of theory using Gaussian 09 software. Subsequently, antechamber within the AMBER software package was employed to develop force field parameters for both substrates.[6,7] Molecular docking was conducted using AutoDock Vina 1.5.6, employing a rigid docking protocol where the enzyme structure remained fixed while substrates explored various conformations.[8] This generated 20 poses for each substrate, ranked based on energy, with the two lowest-energy poses selected for further energy minimizations. The selected poses were solvated in a cubic box with TIP3P water molecules, while ensuring a 2.0 nm distance from the protein surface to the box edge.[9-11] The system's total charge was neutralized by adding $Na^+$ and $Cl^-$ ions to emulate physiological conditions (0.154 M). Electrostatic interactions were computed using the particle mesh Ewald method, and a 1.2 nm cutoff was set for van der Waals and Coulombic interactions. Initial structure energy minimization involved 3000 steps with the steepest descent algorithm. Subsequently, a 100 ns molecular dynamics simulation was performed using the GROMACS 2022 software package with Amber 14 parmbsc1 forcefield.[2-4] Clustering analysis on the 100 ns trajectory yielded a most represented model with a 0.3 RMSD cutoff for each substrate. Frames 10 ns before and after the timestamp from the clustered result were extracted from the trajectory, and the final binding free energy was computed based on these frames using the gmx_MMPBSA module.[12]

**Synthesis of EB-ss-DM1**

*Synthesis of* ***1 (SS-COOH: SS-COOH-3, SS-COOH-16)***

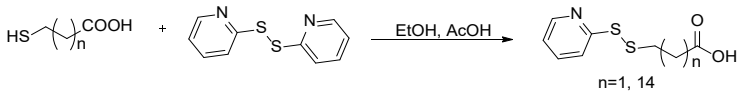


2,2-dithiopyridine (404.6 mg, 1.84 mmol) was dissolved in EtOH (10 mL), and AcOH (50 μL) was added. To the mixture, a solution of 3-mercaptopropionic (104 μL, 1.2 mmol) in EtOH (5 mL) was added dropwise at room temperature. The reaction mixture was stirred overnight. The mixture was concentrated by a rotatory evaporator, and the residue was purified by chromatography. Gradient ethyl acetate and hexane mixture (1/1) were used as eluent. Yield: 39 mg (14.8% yield). ***SS-COOH-16*** was synthesized using a similar method to that of 16-mercaptohexadecanoic acid as the starting material. $^1$H NMR (500 MHz, Chloroform-*d*) δ 8.50 (dt, *J* = 5.0, 1.4 Hz, 1H), 7.75 – 7.64 (m, 2H), 7.23 – 7.14 (m, 1H), 3.08 (t, *J* = 6.8 Hz, 2H), 2.82 (t, *J* = 6.8 Hz, 2H). $^1$H NMR (500 MHz, Chloroform-*d*) δ 8.41 (d, *J* = 4.9 Hz, 1H), 7.68 (d, *J* = 8.0 Hz, 1H), 7.58 (td, *J* = 7.8, 1.9 Hz, 1H), 7.02 (dd, *J* = 7.3, 4.9 Hz, 1H), 2.72 (t, *J* = 7.3 Hz, 2H), 2.28 (t, *J* = 7.4 Hz, 2H), 1.58 (dq, *J* = 24.9, 7.6 Hz, 4H), 1.18 (d, *J* = 4.6 Hz, 23H). (Fig. S8-S9)

*Synthesis of* ***2 (SS-P: SS-P-3, SS-P-16)***

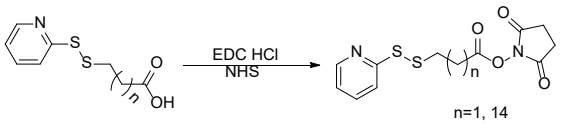


***SS-COOH-3*** (39 mg, 0.18 mmol) was dissolved in 2 mL DCM. 3-(ethyliminomethylideneamino)-*N*, *N*-dimethylpropan-1-amine; hydrochloride (EDC HCl, 42 mg, 0.22 mmol) and NHS (25 mg, 0.22 mmol) were added, and the reaction mixture was stirred at 0 ℃ for 2 h. The mixture was concentrated by a rotatory evaporator, and the residue was purified by chromatography. Gradient ethyl acetate and

hexane mixture (1/1, v/v) were used as eluent. Yield: 16 mg (28.6% yield). ***SS-P-16*** was synthesized using a similar method to that of ***SS-COOH-16*** as the starting material. $^1$H NMR (500 MHz, Chloroform-*d*) δ 8.48 (d, *J* = 4.8 Hz, 1H), 7.71 – 7.62 (m, 2H), 7.11 (td, *J* = 5.4, 2.5 Hz, 1H), 3.18 – 3.03 (m, 4H), 2.83 (s, 4H). $^1$H NMR (500 MHz, Chloroform-*d*) δ 8.42 – 8.35 (m, 1H), 7.67 (d, *J* = 8.1 Hz, 1H), 7.58 (td, *J* = 7.8, 1.8 Hz, 1H), 7.01 (dd, *J* = 7.4, 4.8 Hz, 1H), 2.83 – 2.68 (m, 6H), 2.53 (t, *J* = 7.5 Hz, 2H), 1.72 – 1.57 (m, 4H), 1.31 – 1.15 (m, 22H). (Fig. S10-S11)

*Synthesis of* ***3 (EB-ss-P: EB-ss-P-3, EB-ss-P-16)***

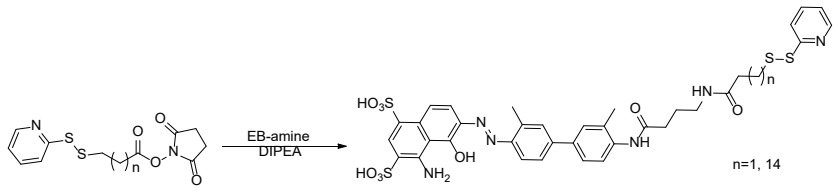


***EB-ss-P-3*** (3.4 mg, 0.011 mmol) was dissolved in 2 mL DMF, then the ***EB-amine*** (6.8 mg, 0.011 mmol) and DIPEA (7 mg, 0.054 mmol) was added, the reaction was stirred overnight. The mixture was precipitated into a mixture of ethyl acetate and hexane (1/1, v/v) three times. *Compound* ***3*** was obtained after vacuum drying. Yield: 5.6 mg (62.2% yield). ***EB-ss-P-16*** was synthesized using a similar method to that of ***SS-P-16*** as the starting material. $^1$H NMR (300 MHz, methanol-$d_4$) δ 8.71 (d, J = 7.5 Hz, 1H), 8.44 – 8.37 (m, 1H), 7.97 (d, J = 2.0 Hz, 1H), 7.88 – 7.82 (m, 2H), 7.57 (dd, J = 8.5, 2.0 Hz, 1H), 7.42 – 7.37 (m, 1H), 7.23 (dd, J = 9.3, 3.9 Hz, 2H), 7.07 (d, J = 9.9 Hz, 1H), 3.68 (d, J = 6.6 Hz, 2H), 3.18 (s, 2H), 3.10 (d, J = 7.1 Hz, 2H), 2.69 (t, J = 7.0 Hz, 2H), 2.48 (s, 3H), 2.23 (s, 3H), 1.91 (t, J = 7.3 Hz, 2H). HRMS (ESI) m/z: calculated for $C_{36}H_{36}N_6O_9S_4$ 824.1427, found [M-H]- =823.1442. HRMS (ESI) m/z: calculated for $C_{49}H_{62}N_6O_9S_4$ 1004.3461, found [M-H]- =1005.3433. (Fig. S12) (Fig S15-S16)

*Synthesis of **EB-amine***

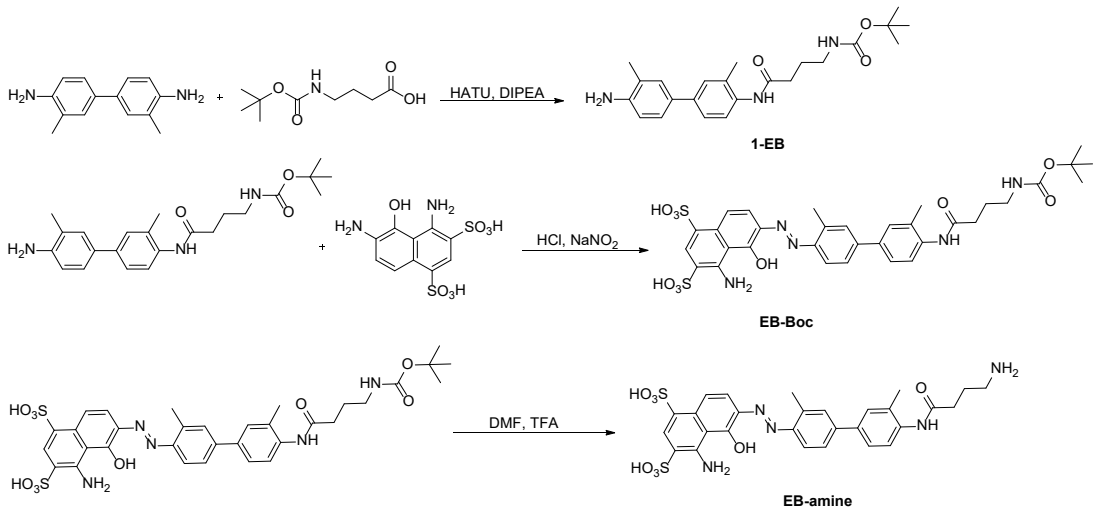


o-Tolidine (2 g, 9.42 mmol) was dissolved in 10 mL DMF in a 50 mL flask. After stirring for 5 min, the 4-((tert-butoxycarbonyl)amino)butanoic acid (1 g, 4.92 mmol), HATU (3.5 g, 9.20 mmol) and *N*, *N*-diisopropylethyl-amine (DIPEA, 3 g, 23.2 mmol) was dissolved in 10 mL DMF, and then dropwise to the mixture. The reaction mixture was stirred for 6h at room temperature. Yellow mixture was washed with water (1 × 100 mL), saturated $NaHCO_3$ aqueous solution (2 × 100 mL), and saturated brine (1 × 100 mL). The organic layer was separated and dried over anhydrous $Na_2SO_4$. The solution was concentrated by a rotatory evaporator, and the residue was purified by chromatography. Gradient ethyl acetate and hexane mixture (3/1, v/v) were used as eluent. Yield: 0.9 g (48.1% yield).

A solution of 4 mL cold 2.0 M HCl was added dropwise to a 10 mL solution of ***1-EB*** (0.9 g, 2.26 mmol) in DMF in a 25 mL flask in an ice bath. After stirring for 15 min, 5 mL of saturated sodium nitrite was slowly added to the reaction mixture and was stirred for another 30 min to obtain a yellow solution. The obtained solution was then added dropwise to the mixture solution of $NaHCO_3$ (1.25 g, 14.9 mmol) and 1-amino-8-naphthol-2,4-disulfonic acid monosodium salt hydrate (1.15 g, 0.55 mmol, dissolved in 4 mL water) in an ice bath. After stirring for another 60 minutes, a purple reaction

mixture was obtained. The reaction mixture was purified by preparative HPLC, and lyophilized to 375 mg purple powder product (yield 22.5%). HRMS (ESI) m/z: [M-H]- calculated for $C_{33}H_{37}N_5O_{10}S_2$ 727.1982, found 726.2053. (Fig. S13)

***EB-Boc*** (375 mg, 0.516 mmol) was dissolved in 6 mL DMF in a 25 mL flask. The Trifluoroacetic acid (TFA, 3 mL, 0.039 mmol) was added. After stirring for 2 hours, the mixture was precipitated into a mixture of diethyl ether three times. ***EB-amine*** was obtained after vacuum drying. Yield: 107 mg (33.1% yield). HRMS (ESI) m/z: calculated for $C_{28}H_{29}N_5O_8S_2$ 627.1458, [M-H]-= found 626.0354. (Fig. S14)

*Synthesis of* ***EB-ss-DM1 (EB-ss-DM1-3, EB-ss-DM1-16)***

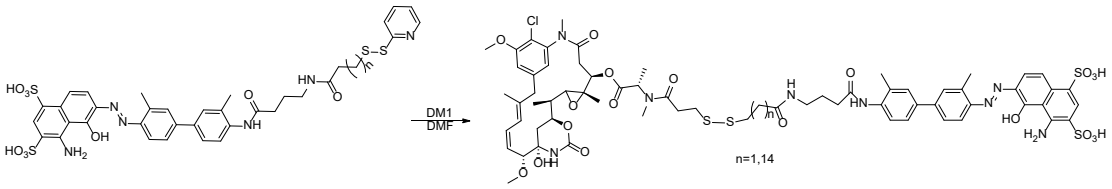


***EB-ss-P-3*** (5.6 mg, 0.007 mmol) was dissolved in 1 mL DMF, then the DM1 (5 mg, 0.007 mmol) was added, and the reaction was stirred overnight. The reaction purified by preparative HPLC using acetonitrile and water (gradient: 5−95% of acetonitrile). The collected purified product was lyophilized and stored at −20 °C. Yield: 3 mg (30.6% yield). ***EB-ss-DM1-16*** was synthesized using a similar method to that of ***EB-ss-P-16*** as the starting material. HRMS (ESI) m/z: calculated for $C_{66}H_{79}ClN_8O_{19}S_4$ 1450.4033, found [2M-H]-= 724.7508. HRMS (ESI) m/z: calculated for $C_{79}H_{105}ClN_8O_{19}S_4$ 1450.4033, found [2M-H]-= 816.3052. (Fig. S17-S18)

## Supplementary results

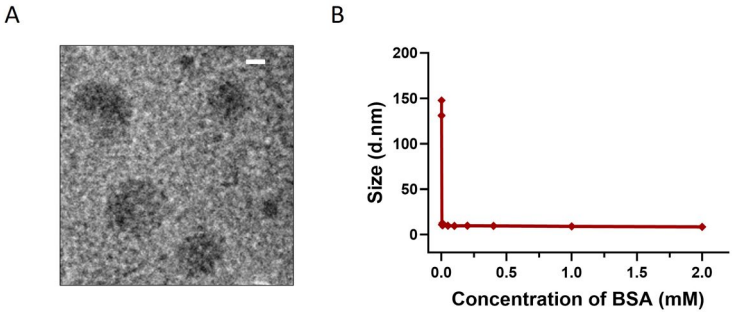


Fig. S1 (A) TEM image of EB-ss-DM1-16. The scale bar represents 50 nm. (B) The size change of EB-ss-DM1-16 with different concentrations of BSA (EB-ss-DM1-16, 0.01 mM in PBS; BSA, 0.001-2 mM in PBS.).

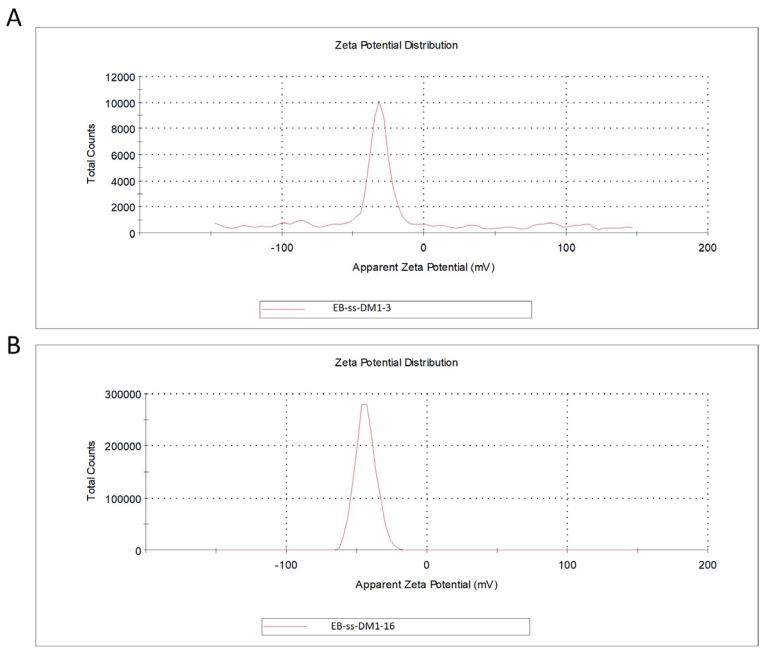


Fig. S2 Zeta potential of (A) EB-ss-DM1-3, (B) EB-ss-DM1-16.

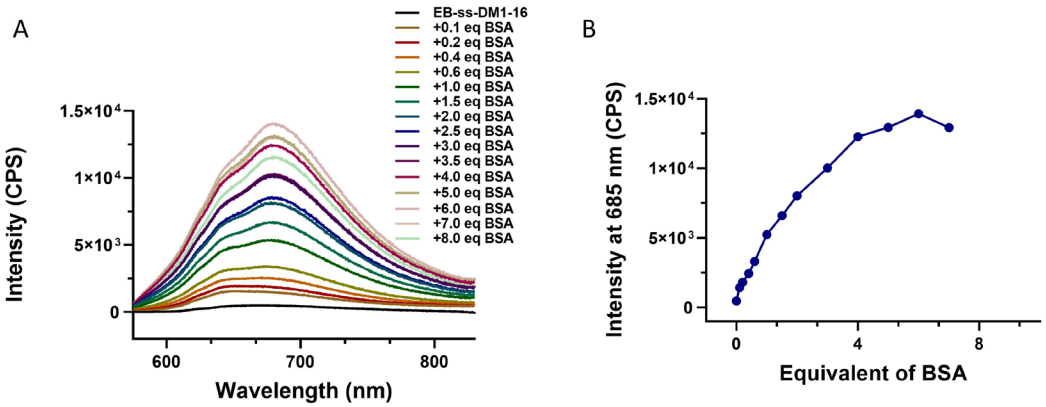


Fig. S3 (A) The emission spectra of EB-ss-DM1-16 and (B) fluorescence intensity at 685 nm (EB-ss-DM1-16, 5 μM in PBS; BSA, 0.5-40 μM in PBS. Excitation: 560 nm).

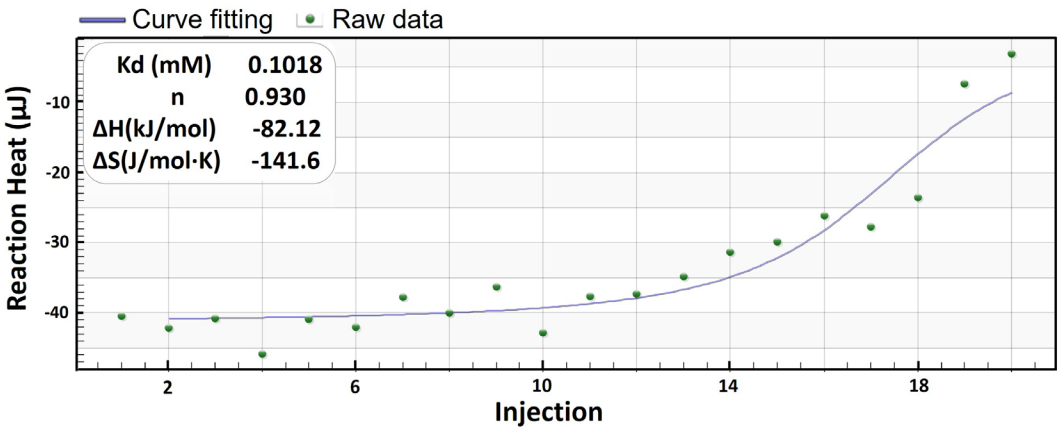


Fig. S4 ITC analysis of the binding affinity of EB-ss-DM1-16 to BSA

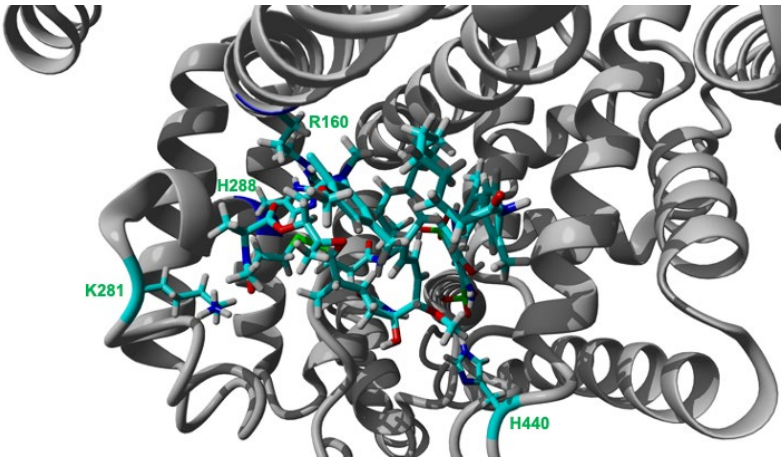


Fig. S5 Predicted structure of the EB-ss-DM1-16/HSA nanocomplex. HSA (gray) is represented in solid

ribbon. EB-ss-DM1 prodrugs and the residues in the binding site of HSA are represented in stick.

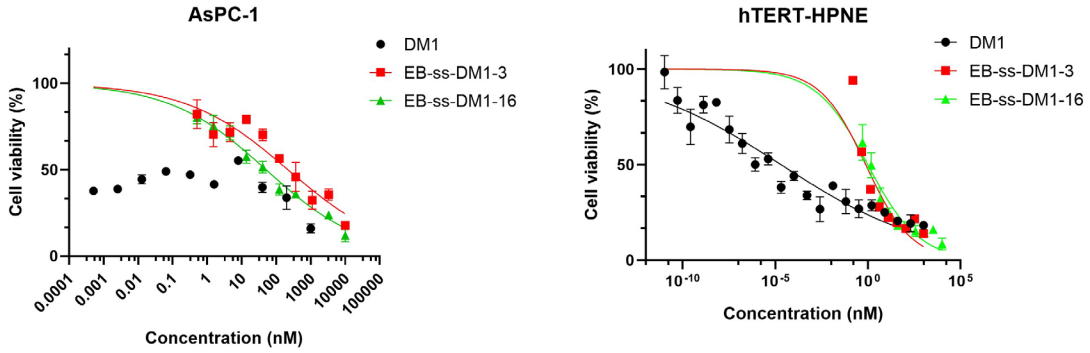


Fig. S6 In vitro cytotoxicities of EB-ss-DM1-3, EB-ss-DM1-16, and DM1 against AsPC-1 and hTERT-HPNE cell.

**Table S1.** $IC_{50}$ of the prodrug values calculated by GraphPad Prism 8.

| Samples | EB-ss-DM1-3 | EB-ss-DM1-16 | DM1 |
|---|---|---|---|
| 4T1 | 17.5 ± 0.5 nM | 37.2 ± 7.4 nM | 0.31 ± 0.13 nM |
| AsPC-1 | 5.9 ± 2.1 nM | 51.3 ± 4.4 nM | Can not be calculated |
| PANC-1 | 0.51 ± 0.02 nM | 1.3 ± 0.1 nM | 0.003 ± 0.001 nM |
| hTERT-HPNE | 0.61 ± 0.28 nM | 1.15 ± 0.52 nM | 0.000029 ± 0.000016 nM |

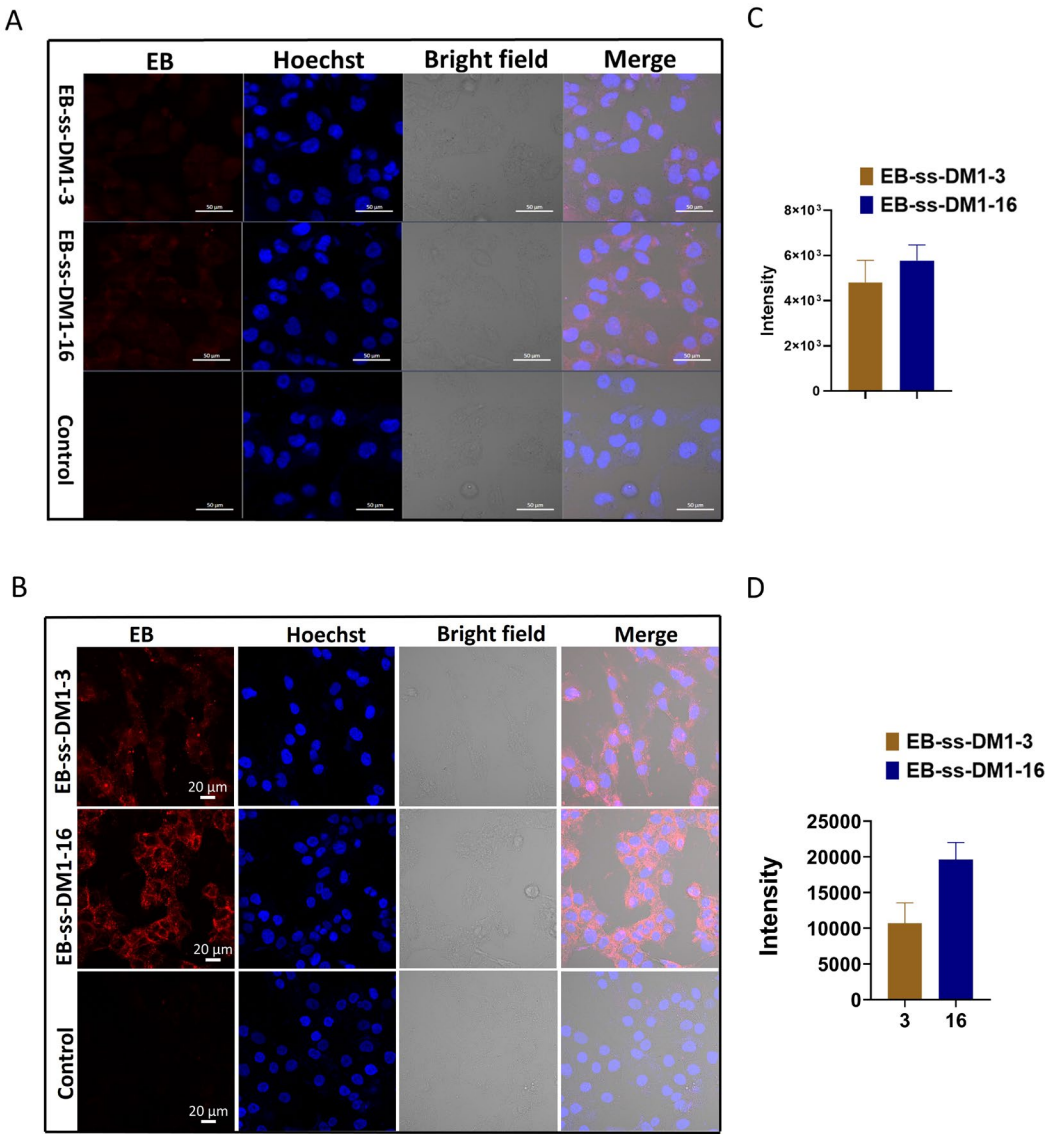


Fig. S7 (A) Confocal microscopic images of PANC-1 cells and (B) h-TERT-HPNE cells treated with 10 μM of EB-ss-DM1-3, EB-ss-DM1-16, and RPMI-1640 media or DMEM medium. Red: EB fluorescence from EB-ss-DM1 prodrugs; Blue: Hoechst 33342 (nuclear stain). (C-D) The average fluorescence intensity of each cell treated with either EB-ss-DM1-3 or EB-ss-DM1-16. (The fluorescence intensity was analysed by ZEISS ZEN 3.8.)

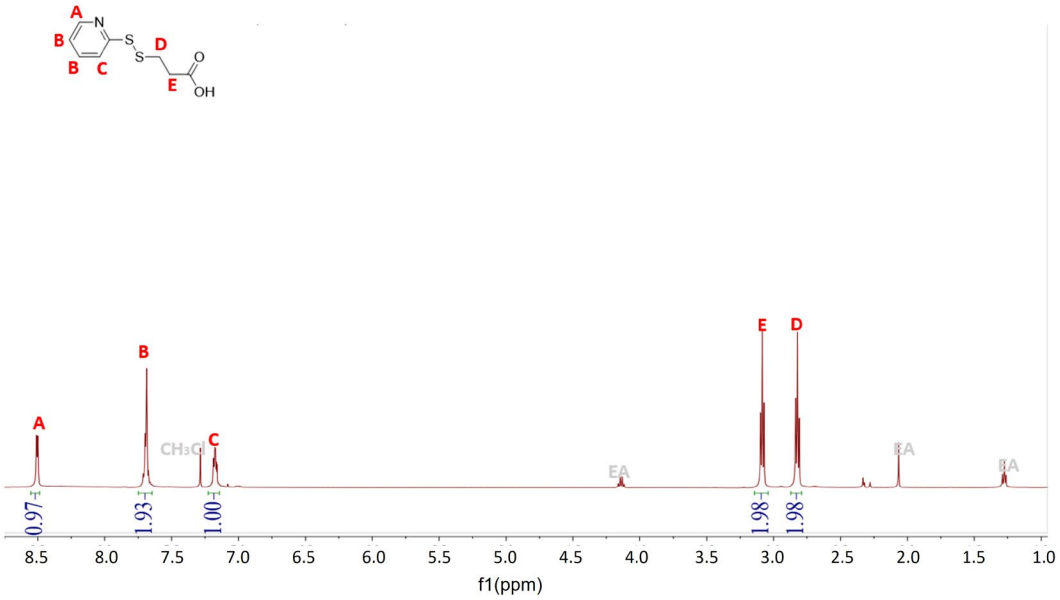


Fig. S8 $^{1}$H NMR of ***SS-COOH-3***

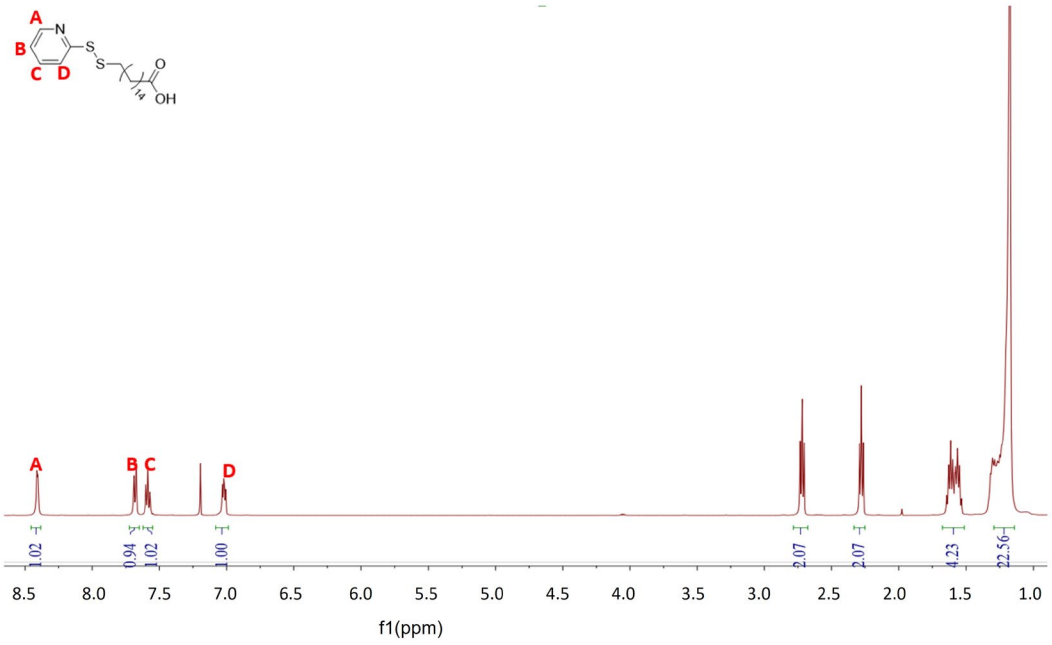


Fig. S9 $^{1}$H NMR of ***SS-COOH-16***

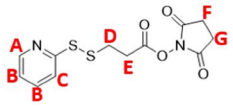


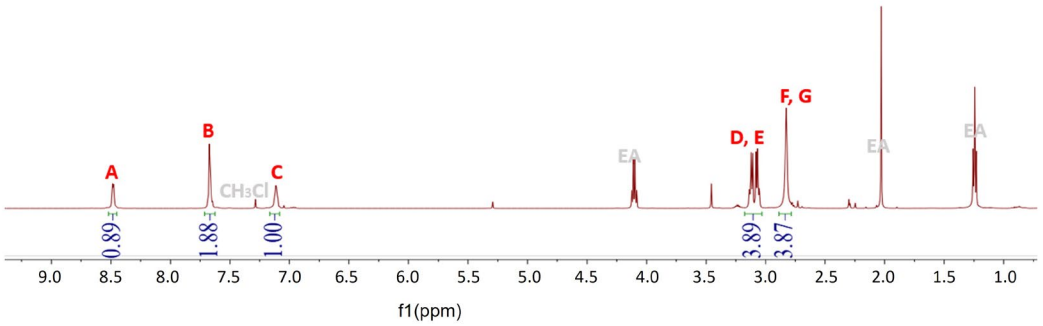


Fig. S10 $^{1}$H NMR of ***SS-P-3***

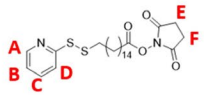





Fig. S11 $^{1}$H NMR of ***SS-P-16***

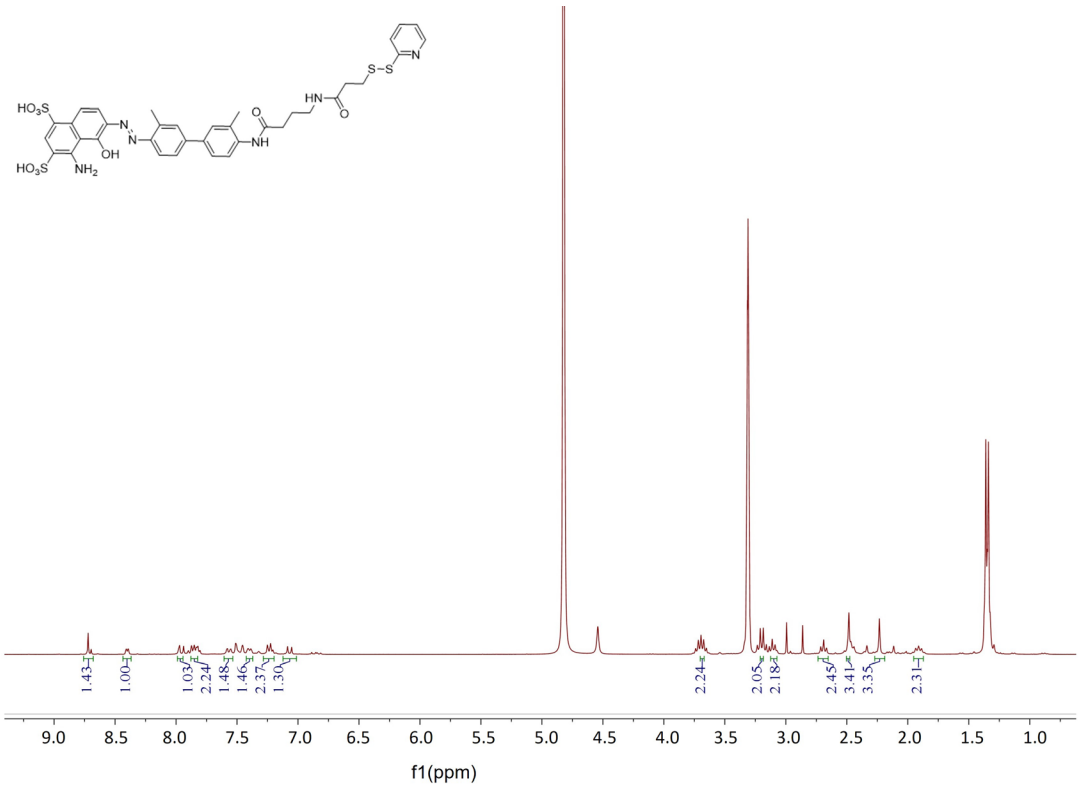


Fig. S12 $^{1}$H NMR of ***EB-SS-P-3***

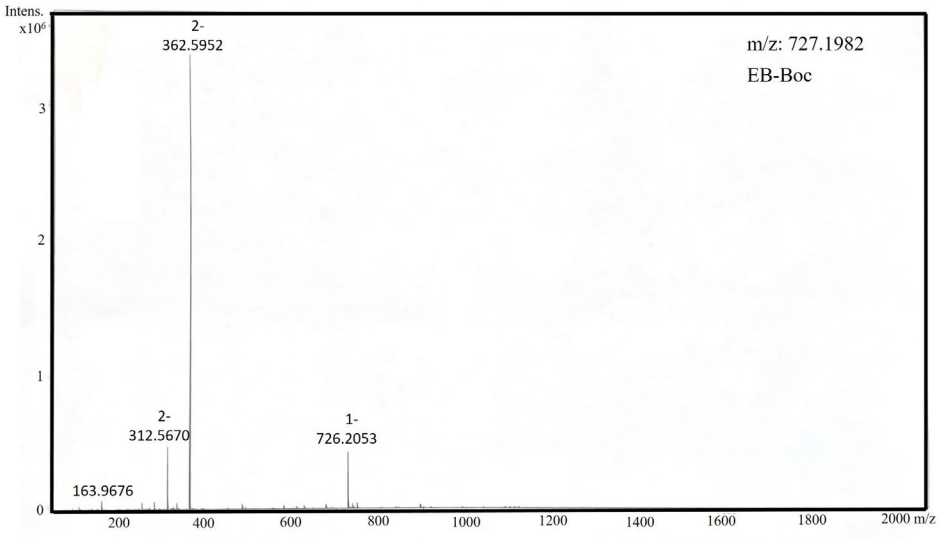


Fig. S13 High-resolution mass spectra of ***EB-Boc***

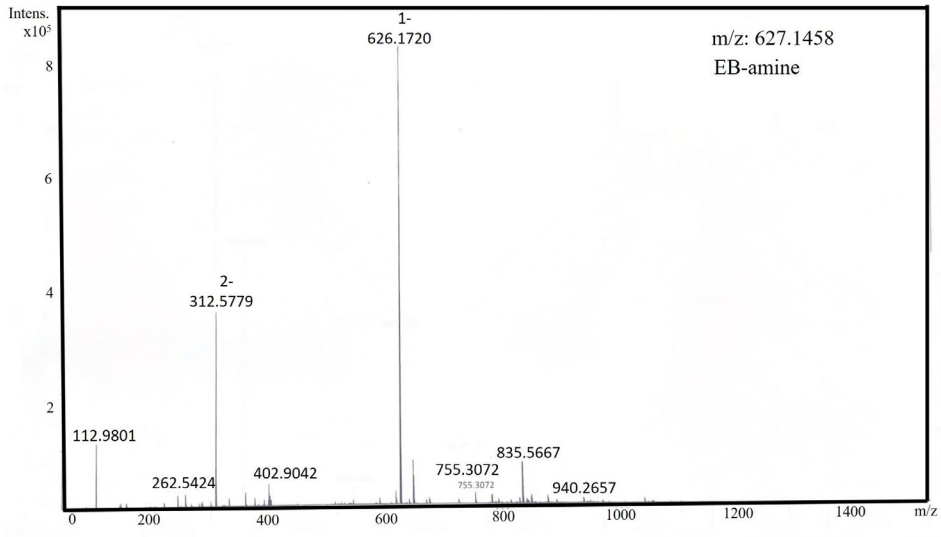


Fig. S14 High-resolution mass spectra of ***EB-amine***

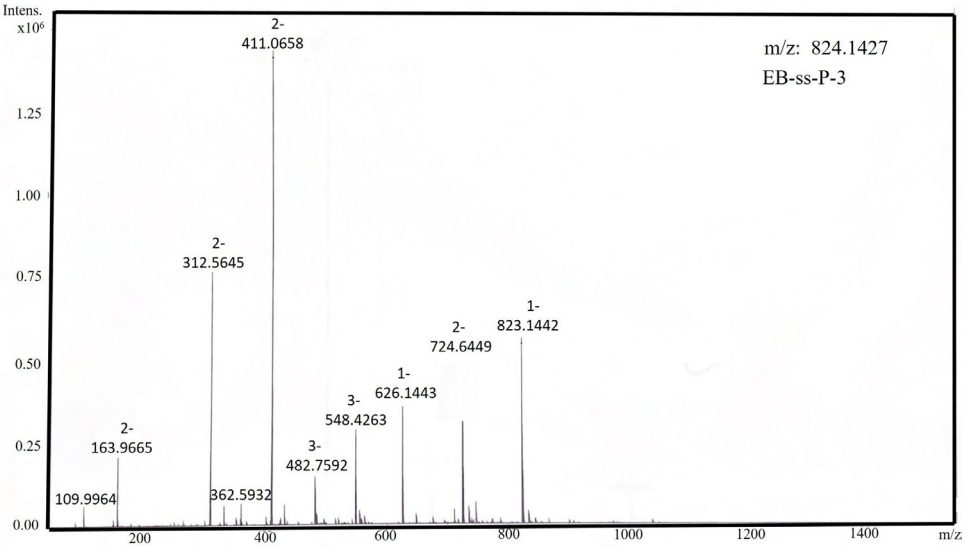


Fig. S15 High-resolution mass spectra of ***EB-ss-P-3***

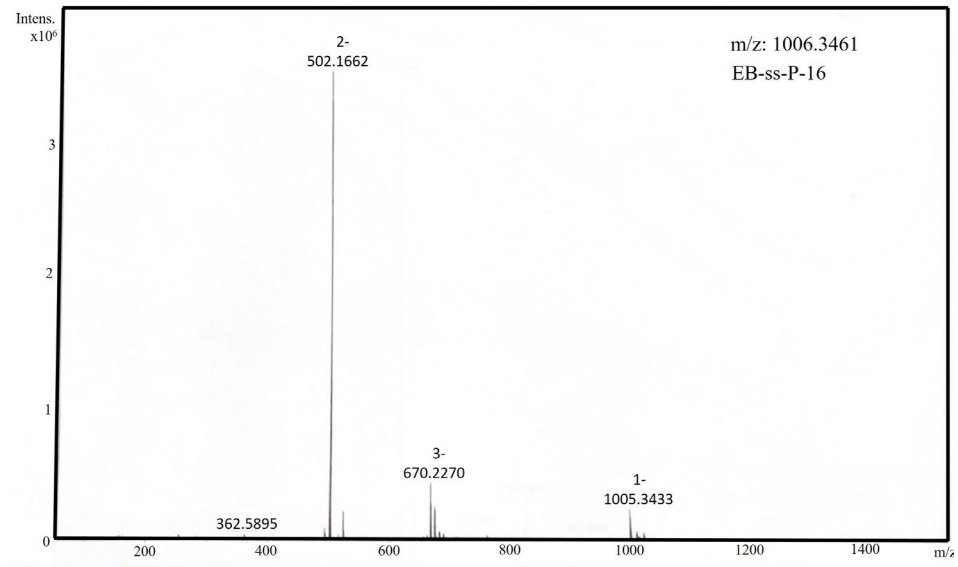

Fig. S16. High-resolution mass spectra of ***EB-ss-P-16***

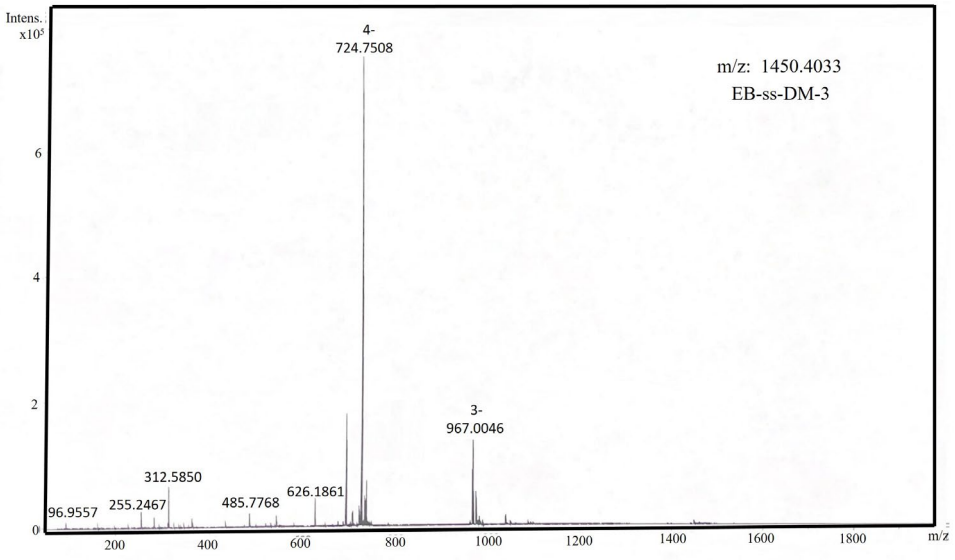


Fig. S17 High-resolution mass spectra of ***EB-ss-DM1-3***

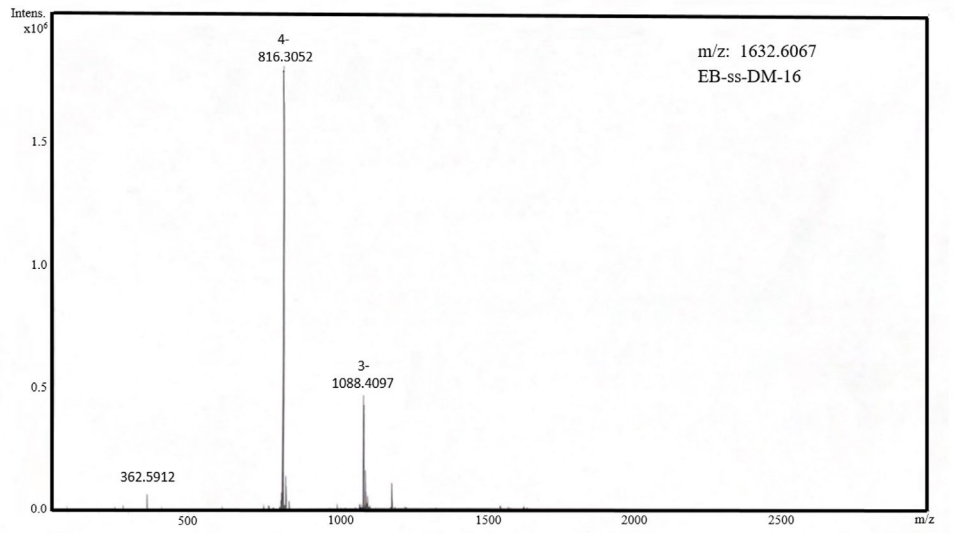


Fig. S18 High-resolution mass spectra of ***EB-ss-DM1-16***

## References


1. J. Ghuman, P. A. Zunszain, I. Petitpas, A. A. Bhattacharya, M. Otagiri, S. Curry, *J. Mol. Biol.*, 2005, **353**, 38-52.

2. P. Bauer, B. Hess, and E. Lindahl. *GROMACS 2022 Manual*. https://doi.org/10.5281/zenodo.6103568

3. M.J. Abraham, T. Murtola, R. Schulz, S. Páll, J.C. Smith, B. Hess, and E. Lindahl, *SoftwareX*, 2015, **1–2** 19–25.

4. I. Ivani, P. D. Dans, A. Noy, A Pérez, I. Faustino, A. Hospital, J. Walther, P. Andrio, R. Goñi, A Balaceanu, G. Portella, F. Battistini, J. L. Gelpí, C. González, M. Vendruscolo, C. A. Laughton, S. A. Harris, D. A. Case, M. Orozco. *Nat. Methods*, 2016, **13**, 55-58

5. Gaussian 09, Revision A.02, M. J. Frisch, G. W. Trucks, H. B. Schlegel, G. E. Scuseria, M. A. Robb, J. R. Cheeseman, G. Scalmani, V. Barone, G. A. Petersson, H. Nakatsuji, X. Li, M. Caricato, A. Marenich, J. Bloino, B. G. Janesko, R. Gomperts, B. Mennucci, H. P. Hratchian, J. V. Ortiz, A. F. Izmaylov, J. L. Sonnenberg, D. Williams-Young, F. Ding, F. Lipparini, F. Egidi, J. Goings, B. Peng, A. Petrone, T. Henderson, D. Ranasinghe, V. G. Zakrzewski, J. Gao, N. Rega, G. Zheng, W. Liang, M. Hada, M. Ehara, K. Toyota, R. Fukuda, J. Hasegawa, M. Ishida, T. Nakajima, Y. Honda, O. Kitao, H. Nakai, T. Vreven, K. Throssell, J. A. Montgomery, Jr., J. E. Peralta, F. Ogliaro, M. Bearpark, J. J. Heyd, E. Brothers, K. N. Kudin, V. N. Staroverov, T. Keith, R. Kobayashi, J. Normand, K. Raghavachari, A. Rendell, J. C. Burant, S. S. Iyengar, J. Tomasi, M. Cossi, J. M. Millam, M. Klene, C. Adamo, R. Cammi, J. W. Ochterski, R. L. Martin, K. Morokuma, O. Farkas, J. B. Foresman, and D. J. Fox, Gaussian, Inc., Wallingford CT, 2016.

6. D. A. Case, T. E. Cheatham, 3rd, T. Darden, H. Gohlke, R. Luo, K. M. Merz, Jr. A. Onufriev, C. Simmerling, B. Wang, R. J. Woods, *J. Comput. Chem.,* 2005, **26**, 1668−1688.

7. A. W. Sousa da Silva and W. F. Vranken, *BMC Res. Notes*, 2012, **5**, 367.

8. O. Trott and A. J. Olson, *J. Comput. Chem.*, 2010, **31**, 455-461.

9. A. D. MacKerell, Jr., D. Bashford, M. Bellott, R. L. Dunbrack, Jr., J. D. Evanseck, M. J. Field, S. Fischer, J. Gao, H. Guo, S. Ha, D. Joseph-McCarthy, L. Kuchnir, K. Kuczera, F. T. K. Lau, C. Mattos, S. Michnick, T. Ngo, D. T. Nguyen, B. Prodhom, W. E. Reiher, B. Roux, M. Schlenkrich, J. C. Smith, R. Stote, J. Straub, M. Watanabe, J. Wiórkiewicz-Kuczera, D. Yin and M. Karplus, *The Journal of Physical Chemistry B*, 1998, **102**, 3586-3616.

10. W. L. Jorgensen, J. Chandrasekhar, J. D. Madura, R. W. Impey and M. L. Klein, *The Journal of Chemical Physics*, 1983, **79**, 926-935.

11. D. J. Price and C. L. Brooks, III, *The Journal of Chemical Physics*, 2004, **121**, 10096-10103.

12. M. S. Valdés-Tresanco, M. E. Valdés-Tresanco, P. A. Valiente and E. Moreno, *Journal of Chemical Theory and Computation*, 2021, **17**, 6281-6291.